Advanced Strain Compensation in MBE-Grown Semiconductor Disk Lasers

Fernando Rinaldi and Susanne Menzel

Strain compensation in disk lasers is described in detail in this article. The analyzed structures are pseudomorphically grown by MBE (molecular beam epitaxy) on GaAs substrates and are designed for an emission wavelength of 920 nm. It is shown that strain compensation is needed to produce reliable laser devices and two different strain compensation strategies are compared.

1. Introduction

Nowadays semiconductor disk lasers are of great importance in virtue of their high output power. In fact, it is common to fabricate devices having an output power of several watts [1, 2]. Furthermore, the free access of the resonator allows intracavity SHG (second harmonic generation) using nonlinear crystals. In this way, the range of emission wavelengths that can be realized using different compound semiconductors is furthermore expanded.

It is clear that such high emission power stretches the semiconductor material close to its stability limit, and different techniques should be used to improve the device performances. One of this methods is the strain compensation, that allows to grow complex disk laser structures that are able to achieve higher output power without showing any degradation.

2. Typical Disk Laser Structures

The structure of the considered disk lasers is basically composed of two parts. The first part is the DBR (distributed Bragg reflector), which is made of an alternating sequence of $AlAs/Al_{0.20}Ga_{0.80}As$ layers, these two materials have the highest refractive index contrast that guarantees no fundamental absorption for the 808 nm pump light. The second part is the active region, which consists of multiple $In_{0.08}Ga_{0.92}As/GaAs$ QWs (quantum wells) separated by GaAs and $Al_{0.20}Ga_{0.80}As$ layers with the respective functions of absorbing the pump light radiation and providing carrier confinement. In order to improve this absorption, a special layer design consisting of a double periodic sequence of layers is employed. In this case the reflectivity spectrum of the resulting DBR exhibits two stop bands, one is used for the emission wavelength, the second one for the pump light.

The MBE pseudomorphic growth of the multilayers, performed on GaAs (001) substrates starts with the active region, and is followed by the DBBR (double band Bragg reflector). This structure is then mounted, in reversed order, on a heat sink and then the substrate is chemically removed. More details about the design, processing, and characterization of the resulting disk laser chips can be found in [2, 3].

3. Disk Laser Strain Compensation

Four samples (a,b,c,and d) are considered in the following sections. The described structures are compressively strained because not only the $In_{0.08}Ga_{0.92}As$ alloy of the 8 nm thick QWs exhibits an in-plane strain ϵ of $-0.57\,\%$, but also the almost unstrained AlAs contributes with an in-plane strain of $-0.15\,\%$. It results that the multilayer tends to introduce dislocations on the [110] and [$\bar{1}$10] directions in order to partially relax the structure. Following [4, 5] one can try to suppress the formation of the misfit dislocations alternating the sign of the strain, in order to minimize the term S defined as

$$S = \left| \sum_{i}^{N} \epsilon_i C_i d_i \right| \qquad \text{with} \qquad C_i = \frac{c_{11i}^2 + c_{11i}c_{12i} - 2c_{12i}^2}{c_{11i}}, \tag{1}$$

where the index i refers to the ith layer of thickness d_i and c_{11i} and c_{12i} are the relative elastic constants in the assumption of cubic crystal material. The reduction of S can be obtained using $GaAs_{1-y}P_y$, because this alloy can easily replace $Al_{0.20}Ga_{0.80}As$ in part of the structure. In fact, for values of y between 0.2 and 0.3, $GaAs_{1-y}P_y$ has a band structure and also a refractive index that properly fit to that purpose [6] just by adjusting the optical thickness.

4. Characterization of the Samples

Different methods are used to characterize the samples. First of all, HRXRD (high resolution x-ray diffraction) measurement are performed on the as grown samples. In fact, symmetric $\omega - 2\theta$ scans relative to the (002) and (004) Bragg reflections provide important informations about the grown structure. For example the (002) allows the accurate investigation of the $AlAs/Al_{0.20}Ga_{0.80}As$ due to the high contrast of the scattering factors given by the presence of aluminum, and, on the other hand, the (004) reflection is more intense and it is more sensitive to strain [7]. HRXRD allows to measure the exact thickness and concentration of the layers in the structure. In particular, the phosphorus concentration of the strain compensating layers and the indium concentration in the QWs can be determined. An example is given in Fig. 1, where the measured and simulated HRXRD spectra relative to the sample d are shown. The simulation is performed considering that for the MBE growth just 4 independent parameters are needed to generate the complex structure [3]. In particular from the (004) spectrum the phosphorus concentration of the GaAsP layer and indium concentration of the QWs can be determined. Using these informations, the strain status of the sample and the value of S can be indirectly calculated. On the other hand, S can be more directly found just by measuring the radius of curvature R of the as grown sample and by using the Stoney's formula. In fact, the curvature of a crystalline multilayer belonging to the cubic system system can be calculated using the relation

$$\kappa = \frac{1}{R} \simeq \frac{6}{C_{\text{sub}} d_{\text{sub}}^2} \sum_i m_i C_i d_i \simeq -\frac{6}{C_{\text{sub}} d_{\text{sub}}^2} \sum_i \epsilon_i C_i d_i, \tag{2}$$

where m_i is the lattice mismatch of the ith layer. The formula above shows that the measurement of the radius of curvature for substrate of fixed thickness (for the used

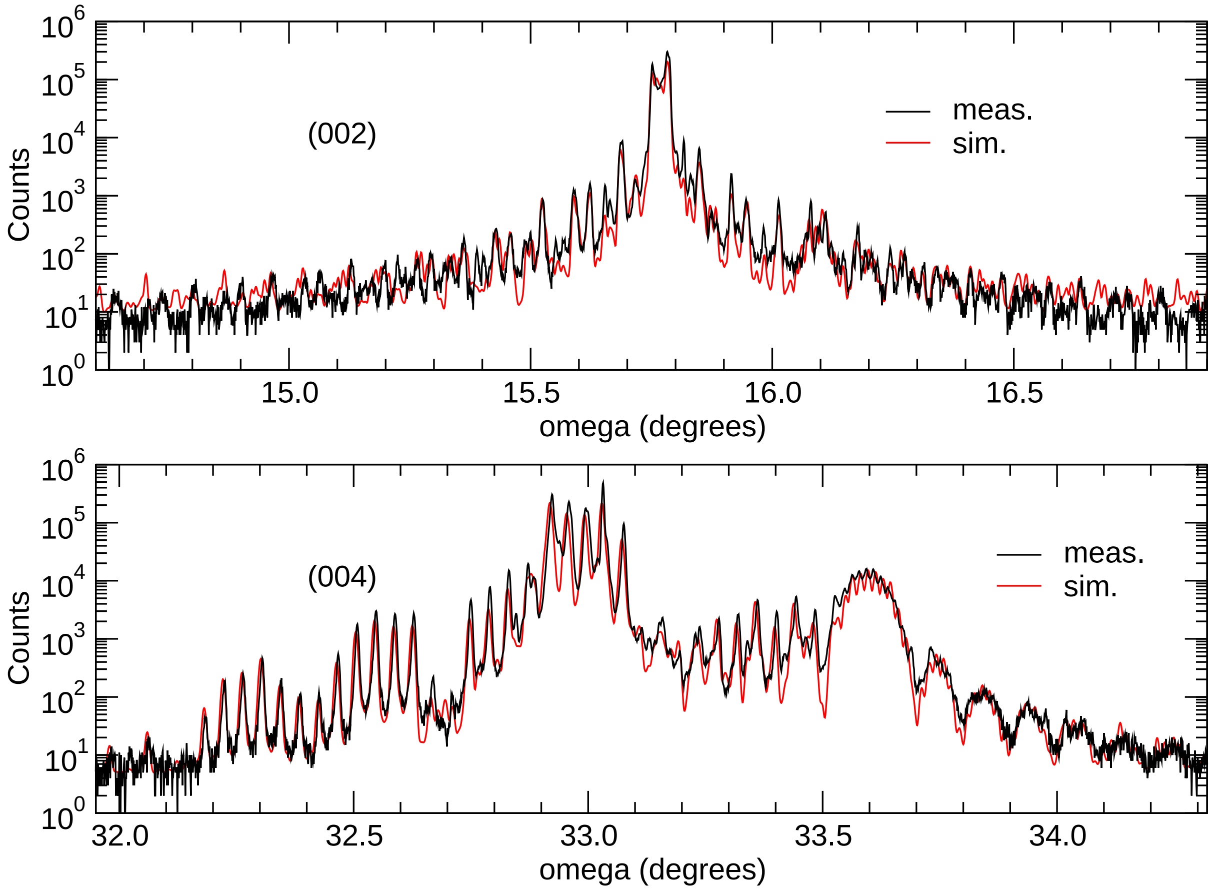

Fig. 1: Symmetric (002) and (004) spectra of the sample *d*. Just 4 independent parameters are needed to describe the complex structure. The phosphorus concentration in the GaAsP layer is 21 %, the indium concentration in the QWs is 8 %.

GaAs substrates $d_{\text{sub}} = 350\,\mu\text{m}$) is directly connected to the strain compensation term S. The curvature κ can be easily obtained experimentally using, for example, HRXRD [3,8], where the angle ω of the substrate diffraction peak, in this case the (004) Bragg reflection, is determined on different sample points lying at different x positions on the intersection line between the sample surface and the diffraction plane. The radius of curvature can be calculated considering the ratio between the increments of Δx and $\Delta\omega$.

As final characterization, the effect of strain compensation on the structure can be visualized by illuminating the prepared laser chip with the 808 nm pump laser light and recording the infrared picture. As can be seen in Fig. 2, orthogonal sets of dark lines are visible on the samples *a* and *b*. The strong suppression of the photoluminescence localized in these lines can be directly observed and it is clearly detrimental for the laser function. In fact, not only a lower efficiency is recorded, but also a shorter device lifetime.

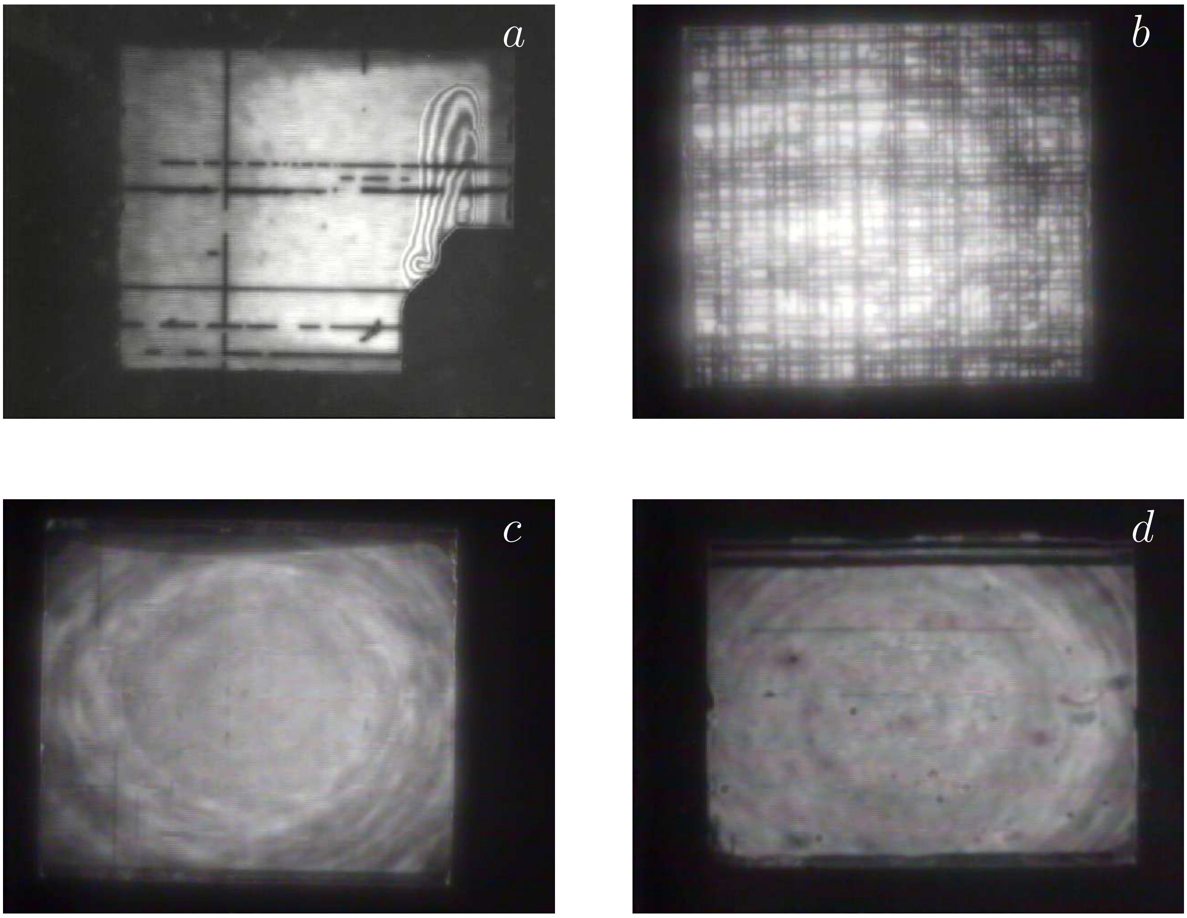

Fig. 2: Infrared pictures of the samples a, b, c, d described in the text. The probes are illuminated with 808 nm light and the dark lines are easily recognizable in an orthogonal pattern. The dimension of each chip is approximately 1 mm×1.5 mm.

5. Discussion

The significant features of the considered four samples are presented in Table 1. The sample a and b are not strain compensated. The two samples differ in the number of QWs and also in the value of the middle concentration of the aluminum alloy in the DBBR. In fact, while in the sample a the aluminum alloy concentration of the 4.2 µm thick reflector is 68 % in the sample b this value is raised to 75 %. As consequence the sample b is more compressively strained than the sample a, as can also be seen by the strong differences in radius of curvature. The abundance of dark lines results in a low efficiency and a reduced lifetime of the device. On the other hand, the samples c and d show even less dark lines than the sample a, even though they incorporate both DBBR with higher aluminum content. The last two samples are in fact strain compensated.

In sample c, the strain compensation layers consist in six 8 nm thick $GaAs_{0.71}P_{0.29}$ situated regularly between the QWs. Instead in sample d, several $GaAs_{0.79}P_{0.21}$ layers having a total thickness of approximately 600 nm, are placed not only between the QWs but also in the DBBR. Considering that the two devices exhibit comparable performances,

Table 1: Summary of data of the 4 samples described in the text.

Sample	Number of QWs	DBBR Al fraction (%)	Radius of curvature (m)	Phosphorus fraction in GaAsP alloy (%)
a	6	69	6.3	0
b	12	75	3.2	0
c	6	75	3.8	29
d	16	72	7.0	21

of more than 5 W output power at 920 nm under an absorbed pump power of 11 and 12 W respectively, one can conclude that the strain arisen from DBBR does not play an important role even though stores most of the elastic energy in the structure. In fact the the radius of curvature of the structure *c* containing a not strain compensated DBBR is much shorter than the one of structure *d* containing a partially strain compensated one.

6. Conclusion

One can prove that even with relatively weak strained $In_{0.08}Ga_{0.92}As$ QWs, that are required for 920 nm emission, disk laser chips take advantage from the introduction of strain compensating layers in the structure, especially when DBBR having an higher content of aluminum are utilized. Almost no dark lines are observed when two different strain compensation scheme are used for devices that show comparable performances. For this reason, more detailed studies are needed to clarify which approach is more convenient in order to further improve the devices.

As conclusion, it is important to emphasize the good efficiency of the strain compensated samples. As example, sample *c* exhibits an output power of 5.4 W at 920 nm for an absorbed 808 nm pump power of 11.0 W and applying SHG achieves 1.6 W at 460 nm [9].

References

[1] M. Kuznetsov, F. Hakimi, R. Sprague, and A. Moradian, "Design and characteristics of high-power (>0.5-W cw) diode-pumped vertical-external-cavity surface-emitting semiconductor laser with circular TEM_{00} beams", *IEEE J. Select. Topics Quantum Electron.*, vol. 5, no. 3, pp. 561–573, 1999.

[2] F. Demaria, *Schicht- und Resonatordesign von Halbleiterscheibenlasern.* Ph.D. thesis, Ulm University, Ulm, 2008.

[3] F. Rinaldi, *MBE Growth and Characterization of Multilayer Structures for Vertically Emitting Laser Devices.* Ph.D. thesis, URL: http://vts.uni-ulm.de/doc.asp?id=6667, Ulm University, Ulm, 2008.

[4] W.D. Nix, “Mechanical properties of thin films”, *Metallurgical Transactions A*, vol. 20A, pp. 2217–2245, 1989.

[5] L.D. Landau and E.M. Lifshitz, *Theory of Elasticity*, Pergamon Press, 1986.

[6] G.D. Clark, Jr. and N. Holonyak, Jr., “Optical properties of gallium arsenide-phosphide”, *Phys. Rev.*, vol. 156, no. 3, pp. 913–924, 1966.

[7] P.F. Fewster, *X-Ray Scattering from Semiconductors*, Imperial College Press, 2000.

[8] V. Holỳ, U. Pietsch, and T. Baumbach, *High-Resolution X-Ray Scattering from Thin Films and Multilayers*, Springer, 1999.

[9] F. Demaria and A. Hein, “Intra-cavity second-harmonic generation of blue 460 nm watt-level emission from optically pumped semiconductor disk lasers”, *Annual Report 2009*, pp. 3–10. Ulm University, Institute of Optoelectronics.